Electronic Supplementary Information

Defect-promoted photo-electrochemical performance enhancement of orange-luminescent ZnO nanorod-arrays

Jan Kegel,[a]* Fathima Laffir,[b] Ian M. Povey,[a] Martyn E. Pemble[a,c]

[a] *Tyndall National Institute, University College Cork, Lee Maltings, Cork, Ireland.*
[b] *Bernal Institute, University of Limerick, Limerick, Ireland.*
[c] *Department of Chemistry, University College Cork, Cork, Ireland.*
* Corresponding author: jan.kegel@tyndall.ie

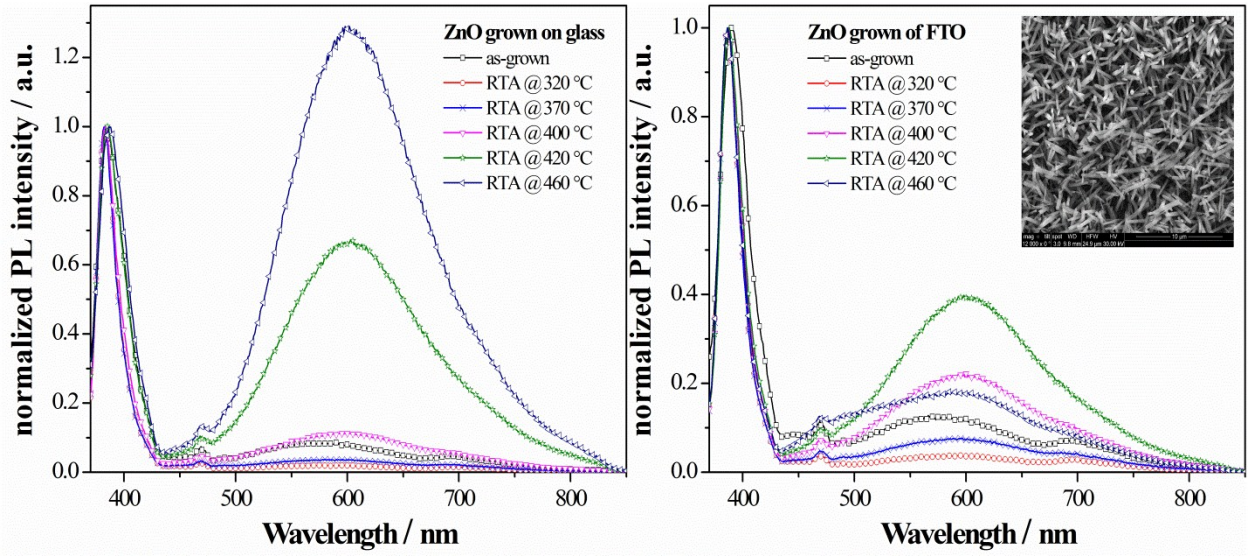

Fig. S1: Annealed ZnO nanorod-arrays grown on different substrates (same seed layer preparation used). Left) ZnO nanorod-arrays grown on ALD seed layer with glass as the substrate. Right) ZnO nanorod-arrays grown on ALD seed layer with FTO as the substrate. When FTO is used as the substrate the orange emission is generally less and occurs/peaks at ca. 30 °C lower temperatures compared to the sample grown on glass. The inset shows a top-view SEM micrograph of the photo-electrode, revealing that the alignment and density is lower for nanorod-arrays grown on FTO/seed layer (compare Fig. 1 of the main text). This may point towards a structural influence on the obtained photo-luminescence spectra.

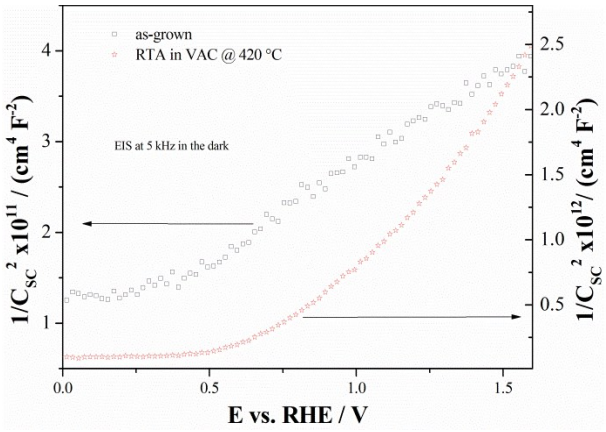

Fig. S2: Examples of Mott-Schottky plots obtained in the dark at 5 kHz of as-grown and RTA treated (vacuum 420 °C) ZnO nanorod-arrays. The frequency of 5 kHz was chosen to reduce the influence of the double-layer capacitance in the electrolyte and slow charge transfer processes (slower time domain). For the as-grown sample a linear dependence of $1/C^2$ from the applied potential is observed, indicating that the band-edges are "pinned" at the semiconductor-electrolyte interface.[1, 2] The Mott-Schottky plot for the sample annealed at 420 °C (strong orange-emission) does not show a linear increase of $1/C_{SC}^2$ with the applied potential. To a lesser extend this behavior has also been observed for the sample annealed at 350 °C (strong band-band recombination and little orange emission – see main text). A non-linear behavior might indicate that the Fermi-level is "pinned" to surface states.[1] Generally the non-linearity reveals that the charge transfer at the semiconductor-electrolyte is more complex than in the case of the as-grown sample. Different charge carrier transfer routes (e.g. holes from the conduction band oxidizing the electrolyte, electron transfer from the electrolyte into defect states) are thereby possible and might contribute to the curved slope in the figure. For the as-grown sample the flatband potential E_{FB} and the donor concentration N_D^+were estimated from the x-axis intercept and the slope of the linear extrapolation (range used for fit 0.5 V – 1.5 V vs. RHE), respectively. The Mott-Schottky equation was used: $1/C_{SC}^2 = (2/(\varepsilon_0\varepsilon_r q N_D^+ A^2))(E_a - E_{FB} - kT/q)$. Where ε_0 is the permittivity of vacuum, ε_r the relative dielectric constant of ZnO (taken as 8.15)[3], q the electron charge, E_a the applied potential, and kT/q the thermal energy ≈ 26 mV. The in this manner calculated donor density and flat-band potential – $7.76 \cdot 10^{19}$ cm^{-3} and -0.27 V vs. RH, respectively – agree well with literature reports.[3-5] Due to the non-linear behavior a meaningful fit was not possible for the sample exhibiting strong orange emission.

Discussion of the energy barrier associated with the kick-out process for the formation of the V_O-Zn_i defect-complex

Based on theoretical calculations of Kim *et al*. the energy barrier E_B for the kick-out process was calculated to be around 1.3 eV.[6] Following the approach presented by Janotti and Van de Walle, the required annealing temperature *T* to overcome this energy barrier can be calculated using:

$$f = f_0 exp\left(\frac{-E_b}{kT}\right)$$

Where *f* is the frequency a defect can travel with (jump of an atom to a near vacancy site or jump of an interstitial to the next interstitial; in good approximation *f* can be taken as 1 s^{-1}), f_0 is a prefactor (in good approximation f_0 can be taken as 10^{13} $s^{-1}$and k is the Boltzmann constant.[7] An energy barrier of 1.3 eV therefore corresponds to an annealing temperature of *ca*. 231 °C. Table S1 lists estimated energy barriers based on the annealing temperatures used throughout the manuscript. As can be seen in Fig. 5 and Fig. 9 of the main text, orange emission occurs for some samples already to a minor degree at temperatures of about 350 °C. The energy barrier associated with this temperature is *ca*. 1.61 eV,

suggesting that the real energy barrier related to the kick-out process leading to the formation of the defect-complex might be higher than was calculated theoretically by Kim *et al*.[6] When the temperature range from 350 °C to 550 °C is taken as the "window" for the stabilization of the defect-complex an energy higher than 1.6 eV + 0.51 eV (energy difference between 550 °C and 350 °C) results in the annihilation of the defect-complex. The energy of 0.51 eV is hereby in good agreement with the binding energy of the complex reported in the literature (0.5 – 0.6 eV).[6, 8]

Table S1. Estimated energy barriers E_b from some annealing temperatures *T* used throughout the study.

T in °C	E_b in eV	Comments
350	1.61	Start of defect formation – minor orange emission for some samples (e.g. Fig. 5 and Fig. 9 of the main text)
450	1.86	Peak of orange emission around this temperature
550	2.12	Temperature at which no orange emission is clearly observed anymore
636	2.37	Annealing temperature associated with the neutral oxygen vacancy[7]

Influence of Xe flash lamp artefacts on photo-luminescence measurements

The fluorescence spectrometer used to record PL and excitation PL spectra includes different pre-set filters for the excitation as well as for the emission port. Whereas different emission filters (e.g. cut off filter 360 nm) were found to have negligible influence, the selection of the excitation filter crucially effects the spectra. Fig. S3 shows the spectrum of the used xenon (Xe) flash lamp as well as PL spectra taken on a defect-rich ZnO sample and on a microscope glass slide. The PL spectra were taken with different excitation filter settings: Filter1 = band-pass filter 250 – 395 nm; Filter 2 = band-pass filter 335 – 620 nm; a combination of Filter 2 and an additional 450 nm short-pass filter. When exciting with *e.g.* 370 nm the PL spectra of both the microscope glass slide as well as the defect-rich sample show significant differences in the emission recorded between 400 nm and 600 nm depending on the filter selected. Especially when Filter2 is selected the emission spectra show strong artefacts in the range 400 nm – 550 nm originating from the Xe flash lamp. However, at 600 nm the differences between the signals recorded with different filter setting are marginal indicating that artefacts have little or no influence in this wavelength range.

By inserting an additional 450 nm short-pass filter into the excitation beam the artefacts for wavelengths > 450 nm can be dramatically reduced. This leaves only a small wavelength range where artefacts can be present (395 nm – ca. 450 nm). This knowledge is essential when examining the entire emission spectra of a sample upon illumination with different excitation wavelengths, as has been done in Fig. S4. The near-band emission (NBE, left panel in Fig. S4) has been recorded using Filter1 and varying the excitation wavelength from 315 nm to 395 nm. Additionally the use of a 400 nm short-pass filter was found helpful in reducing the artefcts around 400 nm. Apart from the NBE associated with the band-band transition and recombination over shallow defects no additional radiative recombination processes could be observed, even when the sample was excited with $h\nu < E_G$ (385 nm and 395 nm).

The deep-level emission (DLE; right panel in Fig. S4) was recorded using Filter1 for excitation wavelengths between 315 nm and 365 nm. Thereafter Filter2 and an additional 450 nm short-pass filter have been used. For the latter filter setting a Xe flash lamp artifact is visible between 450 nm and

470 nm (see also Fig. S3 and related comments). However, the emission shape does not change until 375 nm and is clearly dominated by the orange emission. For 385 nm ($h\nu < E_G$) the orange emission is significantly reduced and diminishes when longer excitation wavelengths are used (≥ 395 nm). The emission shape of the spectra with $h\nu < E_G$ does however not show any additional features.

It is important to note that when using a single excitation wavelength (345 nm in the main manuscript) the influence of artefacts is insignificant as the combination of the 250 – 395 nm band-pass excitation filter and the 360 nm cut-off emission filter (i.e. 360 nm long-pass filter) provides good control over unwanted reflections of the Xe flash lamp. Furthermore the effect of Xe flash lamp artefacts is also low when carrying out excitation PL measurements fixing the emission wavelength to 600 nm (as done in Fig. 7 of the main text). However, a minor influence in these measurements can stem from the characteristic intensity changes/peaks of the Xe flash lamp (e.g. 363 nm, 393 nm, 405 nm, 421 nm, 441 nm *etc*. – see Fig. S3).

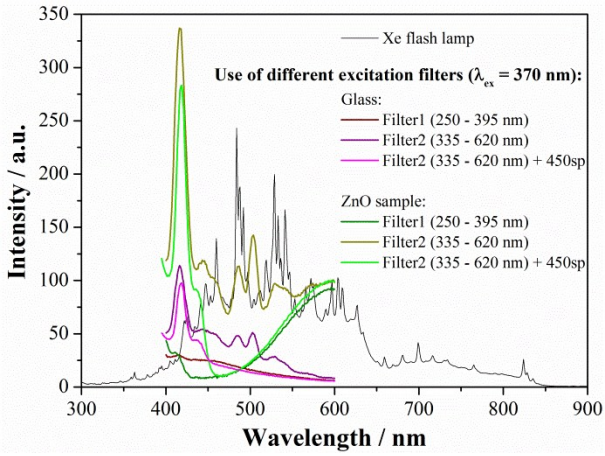

Fig. S3: Comparison of PL spectra recorded with different excitation filter settings showing strong influence of Xe flash lamp artefacts in dependence of the selected excitation filter. An additional 450 nm short-pass filter (450sp) has been used to examine the suppression of artefacts for wavelengths > 450 nm. Note that the artefact visible around 400 nm can be further reduced when an additional 400 nm short-pass is used to filter the excitation beam (not shown).

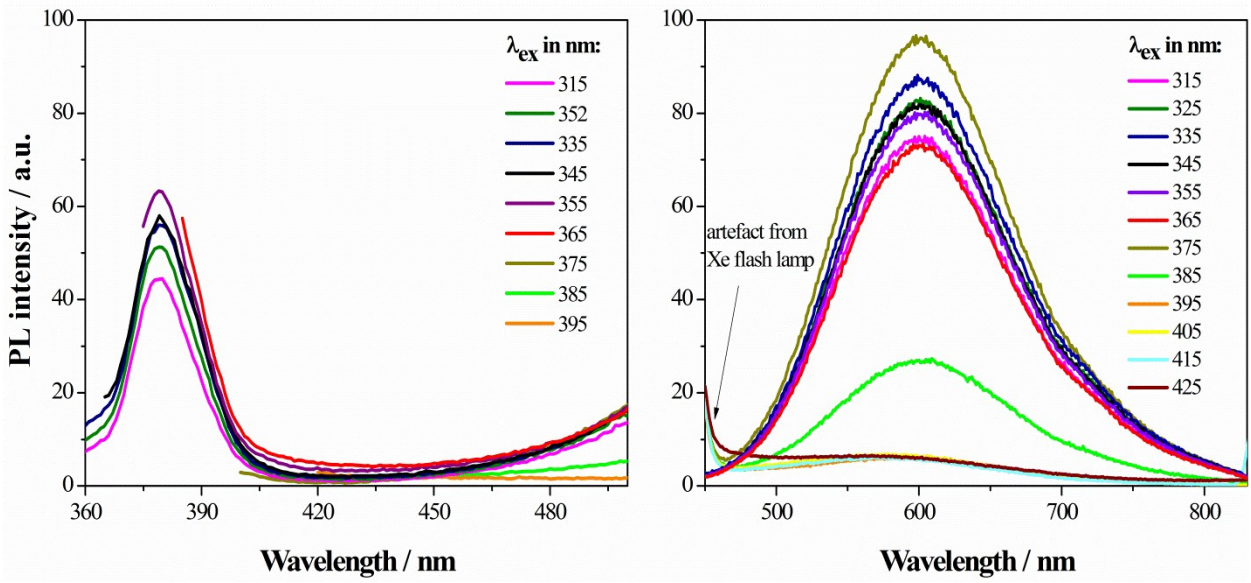

Fig. S4: Near-band emission (left; NBE) and deep-level emission (right; DLE) of defect-rich ZnO nanorod-arrays upon excitation with various wavelengths. Due to the excitation filter settings (see Fig. S3 and related comments) the NBE could only be examined until 395 nm (excitation Filter1). The DLE was recorded using excitation Filter1 until 365 nm and excitation Filter2 and a 450 nm short-pass filter from 375 nm onwards. For the latter filter settings Xe flash lamp artefacts are present at the beginning of the spectra (450 nm - 470 nm)

1. Y. K. Gaudy and S. Haussener, *J. Mater. Chem. A*, 2016, 4, 3100-3114.
2. A. Nakamura, M. Sugiyama, K. Fujii and Y. Nakano, *Japanese Journal of Applied Physics*, 2013, 52, 08JN20.
3. J. Z. Bloh, R. Dillert and D. W. Bahnemann, *Physical Chemistry Chemical Physics*, 2014, 16, 5833-5845.
4. I. n. Mora-Seró, F. Fabregat-Santiago, B. Denier, J. Bisquert, R. n. Tena-Zaera, J. Elias and C. Lévy-Clément, *Applied Physics Letters*, 2006, 89, 203117.
5. V. Sharma, M. Dixit, V. R. Satsangi, S. Dass, S. Pal and R. Shrivastav, *International Journal of Hydrogen Energy*, 2014, 39, 3637-3648.
6. D.-H. Kim, G.-W. Lee and Y.-C. Kim, *Solid State Communications*, 2012, 152, 1711-1714.
7. A. Janotti and C. G. Van de Walle, *Physical Review B*, 2007, 76.
8. Y.-S. Kim and C. H. Park, *Physical Review Letters*, 2009, 102.